Iron overload increases osteoclastogenesis and aggravates the effects of ovariectomy on bone mass

Wang Xiao[1], Fei Beibei[2], Shen Guangsi[1], Jiang Yu[1], Zhang Wen[3], Huang Xi[4] and Xu Youjia[1]

Departments of [1]Orthopaedics, and [2]Gynaecology, The Second Affiliated Hospital of Soochow University, 1055 Sanxiang Road, 215004 Suzhou, China
[3]Department of Orthopaedic Research Institution, Soochow University, 215004 Suzhou, China
[4]Department of Medicine, New York University School of Medicine, 10016 New York, New York, USA

Correspondence should be addressed to X Youjia
Email
xuyoujia@medmail.com.cn

Abstract

Postmenopausal osteoporosis is a metabolic disease associated with estrogen deficiency. The results of numerous studies have revealed the positive correlation between iron accumulation and postmenopausal osteoporotic status. Although the results of previous studies have indicated that estrogen or iron alone have an effect on bone metabolism, their combined effects are not well defined. Using an *in vivo* mouse model, we found that bone mass was minimally affected by an excess of iron in the presence of estrogen. Once the source of estrogen was removed (ovariectomy), iron accumulation significantly decreased bone mass. These effects were accompanied by fluctuations in the level of oxidative stress. To determine whether these effects were related to bone formation or bone resorption, primary osteoblasts (OBs), RAW264.7 cells, and bone-marrow-derived macrophages were used for *in vitro* experiments. We found that iron accumulation did inhibit the activity of OBs. However, estrogen had little effect on this inhibition. In contrast, iron promoted osteoclast differentiation through the production of reactive oxygen species. Estrogen, a powerful reactive oxygen scavenger, suppressed this effect in osteoclasts. Our data provided direct evidence that iron affected the bone mass only in the absence of estrogen. The inhibitory effect of estrogen on iron-induced osteopenia was particularly relevant to bone resorption rather than bone formation.

Key Words
- osteoporosis
- estrogen
- iron
- osteoclasts
- oxidative stress

Journal of Endocrinology (2015) **226**, 121–134

Introduction

Primary type I osteoporosis, also known as postmenopausal osteoporosis (PMO), is a bone disease associated with reduced bone mineral density, disordered bone architecture and increased fragility (Chinese Orthopaedic Association 2009, Van den Bergh *et al.* 2012). Osteoporosis occurs when the bone mass decreases more rapidly than the body can replace it. Approximately 50% of women over 50 years of age suffer from osteoporosis, resulting in staggering financial costs for the USA (Ross 1996, Ray *et al.* 1997). Estrogen deficiency is regarded as the main causative factor in PMO. Withdrawal of estrogen or estrogen deficiency stimulates bone resorption by 90%, while increasing bone formation by 45%, as measured using biochemical markers (Yang *et al.* 2011).

http://joe.endocrinology-journals.org
DOI: 10.1530/JOE-14-0657

Published by Bioscientifica Ltd.

This phenomenon, bone resorption outpacing bone formation, cannot be explained by estrogen deficiency alone (Huang *et al.* 2013). Therefore, we examined whether estrogen shortage is the sole factor in the development of PMO or if other risk factors are involved.

Iron overload has recently been linked to abnormalities in bone metabolism, including osteopenia, osteoporosis, and osteomalacia (Matsushima *et al.* 2001, Guggenbuhl *et al.* 2005). Osteoporosis occurs frequently in disorders associated with an excess of iron, such as thalassemia and hereditary hemochromatosis (Mahachoklertwattana *et al.* 2003, Vogiatzi *et al.* 2006). Most importantly, iron accumulation, a recently observed clinical phenomenon in postmenopausal women, might be involved in the pathogenesis of PMO (Kim *et al.* 2012). Menses is a critical pathway of iron excretion while menopause is a natural aging process that occurs as a woman passes from the reproductive to the non-reproductive years (Milman & Kirchhoff 1992, Riggs *et al.* 2002). Because of physiological amenorrhea, postmenopausal women experience an excess of iron. Although this iron status is considered to be within the normal physiological range, PMO has been linked to increased iron storage, a normal but not necessarily healthy process (Kim *et al.* 2013). Although there was no report of the relationship between iron and osteocytes, inhibition of osteoblastogenesis and stimulation of osteoclastogenesis caused by iron had been reported (Jia *et al.* 2012, He *et al.* 2013) and reactive oxygen species (ROS) were involved in iron-induced osteopenia (Li *et al.* 2012). ROS attenuate osteoblastogenesis, decrease osteoblast/osteocyte lifespan, and are required for osteoclast generation, function, and survival (Khosla *et al.* 2012). Estrogen has been shown to increase markers of oxidative stress in bone (Khosla *et al.* 2012). We propose the hypothesis that estrogen deficiency and increased iron levels are the main and secondary risk factors for PMO respectively. We speculate that iron accumulation aggravates PMO in the absence of estrogen. Furthermore, this deterioration would be suppressed if estrogen is restored using hormone replacement therapy.

In previous work, we established a male mouse model to observe the influence of iron on oxidative stress and bone resorption *in vivo* (Jia *et al.* 2012). In addition, we treated a murine macrophage cell line, RAW264.7 with ferric ions to test their activity (Jia *et al.* 2012). We found that iron promotes osteoclast differentiation and bone resorption. Using the fluorescent probe dichlorodihydro-fluorescein diacetate (DCFH-DA), we examined oxidative stress as the underlying cause of iron-induced enhanced osteoclast function and increased osteoclast differentiation. Our results confirmed that these effects were regulated by the level of reactive oxidative species (ROS) (Li *et al.* 2012).

To examine the combined action of estrogen and iron on bone metabolism, especially the role of iron in PMO, we established an ovariectomized, iron-treated female mouse model. We performed experiments on primary osteoblasts (OBs), bone-marrow-derived macrophages (BMMs), and RAW264.7 cells to elucidate the mechanism underlying the development of PMO. We propose the hypothesis that the NF-κB signaling pathway may be involved in this development. This pathway is activated by virtually all stimuli that affect NF-κB including the receptor activator of NF-κB ligand (RANKL), the master osteoclastogenic cytokine and ROS (Ha *et al.* 2004, Lee *et al.* 2005). Free iron produces ROS through Fenton reactions, and estrogen is a well characterized antioxidant (Kim *et al.* 2006, Nakrst *et al.* 2011). Our analysis of the combined action of estrogen and iron may further our understanding of PMO pathogenesis.

Materials and methods

Animal experiments

All animal experiments were approved by the animal care committee of Soochow University. Two-month-old ICR female mice were divided into four groups ($n=6$/group). Two groups of mice were bilaterally ovariectomized and received intraperitoneal injections of normal saline (OVX) or 40 mg/kg ferric ammonium citrate (FAC) (F+OVX) three times a week for 2 months. The feed was decreased after ovariectomy for weight control. The Control (Con) and F groups, considered as sham operation groups, received identical normal saline and FAC treatments, but their ovaries were not excised. All mice were killed 2 days after the last treatment, and the body weight of all mice was measured.

Blood was collected from the dead mice and then centrifuged at 1000 ***g*** for 10 min in order to acquire the serum. Aliquots of serum were stored at −80 °C for future analysis. BMMs were immediately extracted from one of the two femurs. The other femur from each mouse was scanned using micro-CT. The femurs and livers were then fixed in 10% buffered formalin at 4 °C for Prussian blue staining.

Culture of OBs

Primary OBs derived from the calvaria of 1-day-old ICR mice were obtained as described previously (Suda *et al.* 1997). OBs were maintained in phenol-red-free α-MEM

http://joe.endocrinology-journals.org
DOI: 10.1530/JOE-14-0657

Published by Bioscientifica Ltd.

(Gibco) supplemented with 10% fetal bovine serum (FBS) (HyClone, Logan, UT, USA), 100 units/ml penicillin and 100 μg/ml streptomycin in a humidified atmosphere of 5% CO_2 at 37 °C. The medium was replaced every 2 days. After reaching 70% confluence, the cells were detached using 0.05% trypsin and re-plated in either 55-cm^2 dishes or 12-well plates (3.8 cm^2 wells) at a density of 1×10^4 cells/cm^2. The medium was replaced with serum-free medium containing 0 nM or 10 nM estradiol (E_2) (Krum *et al*. 2008). Then deionized water or 10 μM FAC were used as intervention reagents (Messer *et al*. 2009). Throughout the culture period, 25 μg/ml ascorbic acid, 10 mM sodium β-glycerolphosphate, and 100 nM dexamethasone were supplied to the cells.

Culture of osteoclasts

Murine RAW264.7 macrophage cells were plated in 55-cm^2 dishes or in 96-well plates at 3×10^3 cells/well. RAW264.7 cells were cultured in phenol-red-free α-MEM/10% FBS containing 100 ng/ml RANKL (PeproTech, Rocky Hill, NJ, USA) for 4 days at 37 °C and 5% CO_2. Serum-free medium containing deionized water, E_2, or FAC was supplied to cells during the last 2 days of culture. The method of intervention was the same as for the experiments on OBs.

BMMs were isolated from the femurs by flushing the bone marrow cavity with phenol-red-free α-MEM. Isolated cells were then centrifuged. The medium was replaced with ammonium-chloride-potassium buffer (pH 7.4, 0.1 mM NH_4Cl, 0.1 mM EDTA, and 1 mM K_2CO_3) for 30 s at room temperature to remove the red blood cells. Cells were cultured for 24 h in α-MEM/10%FBS. To generate osteoclast precursors, the non-adherent cells were collected and then cultured for 3 days in the presence of 30 ng/ml of macrophage colony-stimulating factor (M-CSF; PeproTech). The floating cells were discarded and adherent cells were considered to be BMMs. BMMs were cultured in α-MEM containing 30 ng/ml M-CSF and 50 ng/ml RANKL for 5 days.

Cell proliferation assay

Cell proliferation was analyzed using the Cell Counting kit 8 (Dojindo, Tokyo, Japan). RAW264.7 cells were detached and seeded into 96-well plates at a density of 3×10^3 cells/well. After 24 h, cells were treated with FAC at various concentrations (12, 25, 50, 100, and 200 μM, 100 μl/well) or E_2 (1, 10, 10^2, 10^3, and 10^4 nM, 100 μl/well) and they were then incubated for another 24 h. The optical density (OD) of each group was measured at 450 nm using a BioTek microplate reader.

Alkaline phosphatase, alizarin red staining and alkaline phosphatase activity

OBs were treated with FAC and E_2 for 3 days and were then stained using alkaline phosphatase (ALP) following the manufacturer's instructions (Beyotime, Shanghai, China). For alizarin red staining, cells were treated according to the experimental design. After 14 days, Cells were fixed and added with Alizarin Red-S solution (Beyotime) for 30 min. Then mineralized nodules were photographed. Cultured cells were seeded in 12-well plates and treated with FAC and E_2. After 10 days, cells were lysed with cell lysis buffer and centrifuged at 250 ***g*** for 5 min. Aliquots of supernatant were collected to measure ALP activity and protein concentration by using an ALP kit (Jiancheng, Nanjing, China) and a BCA protein assay kit (Beyotime) respectively. The OD was measured at a wavelength of 520 nm by using the BioTek microplate reader.

Tartrate-resistant acid phosphatase staining

To estimate the number of differentiated osteoclasts from bone marrow and RAW264.7 cells, they were stained with tartrate-resistant acid phosphatase (TRAP). Briefly, cells were fixed in 3.7% formaldehyde for 10 min and then incubated for 60 min at 37 °C in the dark with a solution containing sodium nitrite, Fast Garnet GBC, acetate, naphthol AS-BI phosphoric acid, and tartrate from the Leukocyte Acid Phosphatase Assay kit (Sigma) following the manufacturer's instructions. Trap-positive multinucleated cells (MNCs) containing three or more nuclei were scored using light microscopy. The data are expressed as the mean ± S.D. of three samples.

Resorption pit assay

RAW264.7 cells were detached from the flask by using a trypsin/EDTA solution and were then resuspended as a single cell suspension. Cells were re-plated in Osteo Assay Surface 24-well plates (Corning, Corning, NY, USA) at a density of 2.5×10^4 cells/well. α-MEM/10% FBS containing 100 ng/ml RANKL was added to each well. Plates were incubated at 37 °C in a humidified atmosphere of 5% CO_2 for 7 days. The serum-free medium was changed and reagents were added on day 4. The medium was aspirated from the wells on day 7 and 400 μl of 10% bleach solution was added for 5 min. The wells were washed twice in distilled water. Individual pits were examined in dry wells by using a light microscope. The number of pits and the object area/total area were measured using Image-Pro Plus version 6.0 Software (Media Cybernetics, Warrendale, PA, USA).

http://joe.endocrinology-journals.org
DOI: 10.1530/JOE-14-0657

Published by Bioscientifica Ltd.

Measurement of intracellular ROS level

OB and RAW264.7 cells were cultured and treated in 96-well plates. On the last day of culture, cells were incubated in the dark at 37 °C in serum-free medium containing 10 μM DCFH-DA (Beyotime) for 20 min. The cells were washed three times in serum-free medium to remove extracellular DCFH-DA. Cells were immediately examined using a fluorescent microscope. The OD was measured using a multi-detection reader at excitation and emission wavelengths of 488 and 525 nm respectively.

Micro-computed tomography analysis

The distal region of the left femur was subjected to three-dimensional micro-computed tomography (micro-CT) analysis. Bones were analyzed on a SkyScan 1172 high-resolution micro-CT scanner (SkyScan, Aartselaar, Belgium) using a 9-μm voxel size, 59 KVp, 127 μA, and 0.4° rotation step. The measured volumes of the cortical and trabecular regions of interest (ROIs) were obtained using a utility of the processing system. Trabecular ROIs extended from 50 μm proximally to the end of the distal growth plate over 1.7 mm toward the diaphysis. Cortical ROIs were 1.7 mm segments of the femoral middle-diaphysis. Cortical ROIs were defined by digitally subtracting the respective trabecular ROIs from the whole bone volume. All ROIs were drawn semiautomatically. Bone mineral density measurements were performed on cortical and trabecular volumes after segmentation of the bone voxels by using the global threshold, including only bone slices. Cone-beam CT Reconstruction Software version 2.6 was used to perform three-dimensional reconstructions and data analyses. The following trabecular and cortical parameters were analyzed: bone volume/total volume (BV/TV), trabecular number (Tb.N), trabecular separation (Tb.Sp), trabecular thickness (Tb.Th), trabecular bone pattern factor (Tb.Pf), structure model index (SMI), cortical volume, cortical surface, and cortical thickness.

Quantitative RT-PCR analysis

Total RNA was extracted from OB and RAW264.7 cells and was reverse-transcribed into cDNA by using a reverse transcription kit (Invitrogen) following the manufacturer's instructions. The cDNA was mixed with SYBR Green Supermix (Bio-Rad) and primers for runt-related transcription factor 2 (*RUNX2*),transcription factor 7 (*SP7*), bone γ-carboxyglutamate protein (*BGLAP*), *TRAP5*, cathepsin k (*CTSK*), matrix metallopeptidase 9 (*MMP9*), or calcitonin receptor (*CALCR*) respectively. The primers used are listed in Table 1. Each experiment was performed in duplicate and the results were standardized to glyceraldehyde 3-phosphate dehydrogenase (*GAPDH*). All primers were purchased from Sangon (Shanghai, China). Data are expressed as the fold-change relative to the control.

Measurement of ferritin, oxidative stress, and markers of bone turnover in serum

Serum ferritin was measured using a mouse ferritin ELISA kit (Abnova, Taipei, China) according to the manufacturer's protocol. Bone turnover markers including ALP, osteocalcin, C-terminal telopeptide of type 1 collagen (CTX), and TRAP5b were analyzed. ELISA kits for osteocalcin, CTX, and Trap5b were purchased from R&D, while the ALP kit has been previously described. Absorbance at 450 nm was measured for the contents of each well.

Table 1 Primers used for quantitative RT-PCR

Gene	Accession no.	Primers (forward/reverse)
RUNX 2	NM_001145920	(F) 5′-AACTTCCTGTGCTCCGTGCTG-3′ (R) 5′-TCGTTGAACCTGGCTACTTGG-3′
SP7	NM_130458	(F) 5′-AGGAGGCACAAAGAAGCCATAC-3′ (R) 5′-GATGCCTGCCTTGTACCACGAGC-3′
BGLAP	NM_007541	(F) 5′-GGACCATCTTTCTGCTCACTCTG-3′ (R) 5′-GTTCACTACCTTATTGCCCTCCTG-3′
TRAP5	NM_001102405	(F) 5′-TACCTGTGTGGACATGACC-3′ (R) 5′-CAGATCCATAGTGAAACCGC-3′
CTSK	NM_007802	(F) 5′-TGTATAACGCCACGGCAAA-3′ (R) 5′-GGTTCACATTATCACGGTCACA-3′
MMP9	NM_013599	(F) 5′-TCCAGTACCAAGACAAAG-3′ (R) 5′-TTGCACTGCACGGTTGAA-3′
CALCR	NM_007588	(F) 5′-TCAGGAACCACGGAATCCTC-3 (R) 5′-ACATTCAAGCGGATGCGTCT-3′

BGLAP, bone γ-gamma carboxyglutamate protein; *CALCR*, calcitonin receptor; *CTSK*, Cathepsin K; *MMP9*, matrix metallopeptidase 9; RT-PCR, real-time polymerase chain reaction; *RUNX2*, runt-related transcription factor 2, *SP7*, transcription factor SP7; *TRAP5*, tartrate-resistant acid phosphatase.

http://joe.endocrinology-journals.org
DOI: 10.1530/JOE-14-0657

Published by Bioscientifica Ltd.

The plate reader was calibrated according to the manufacturer's specifications. Oxidative stress markers, including malondialdehyde (MDA) and superoxide dismutase (SOD), were detected in the serum by using the MDA assay kit and SOD activity assay kit respectively. ROS will alter the level of SOD and MDA (Hohn *et al*. 2013). Both of the kits were purchased from Jiancheng. The ODs of MDA and SOD were measured at wavelengths of 532 and 450 nm respectively.

Western blot analysis

To analyze the level of NF-κB, whole-cell, cytoplasmic, and nuclear proteins were extracted. Nuclear proteins were extracted using the NucBuster Protein Extraction kit (Novagen, Rockland, MA, USA). Briefly, 2×10^7 RAW264.7 cells were lysed with 150 μl of reagent 1 to remove cytoplasmic proteins. The pellet was resuspended in 1 μl of 100× Protease Inhibitor Cocktail, 1 μl of 100 mM DTT, and 75 μl of reagent 2. The nuclear protein extracts were collected using centrifugation at 16 000 ***g*** for 5 min at 4 °C. A total of 40 μg of protein was mixed with 5×SDS–PAGE Sample loading buffer (Beyotime), boiled at 100 °C for 5 min. Proteins were transferred to PVDF membranes by electroblotting. The membranes were blocked using 5% non-fat dry milk in TBST for 1.5 h and then probed with anti-P50 (1:5000, Millipore, Billerica, MA, USA), anti-P65 (1:2000, Millipore), anti-IkBα (1:1000, Cell Signaling Technology, Danvers, MA, USA), anti-PIkBα (1:1000, Cell Signaling Technology), anti-histone 3 (1:5000, Millipore). Primary antibodies were detected using the DyLing TM800 Labeled Antibody to Rabbit/Mouse IgG (HtL) (1:10 000, KPL, Gaithersburg, MD, USA). Bound complexes were measured using the Odyssey Infrared Imaging System.

Statistical analysis

All the results are presented as the mean±S.D. The differences between the experimental groups were evaluated using one-way ANOVA followed by Bonferroni post tests to allow for multiple comparisons. Statistical analyses were performed using the SPSS 19.0 Software. $P<0.05$ was considered statistically significant.

Results

Osteopenia in mice is associated with iron accumulation and estrogen deficiency

As shown in Fig. 1A, ovariectomized mice fed the control diet showed little weight increase during the period of the experiment. FAC treatment (1.2 g/kg per week) over a 2-month period resulted in a marked iron accumulation in the liver, the largest ferritin reservoir. We stained the liver and bone sections by using Prussian blue, which indicated that iron was deposited in both the liver and bone marrow (Fig. 1B and C). Serum ferritin, a classic marker of iron storage, appeared to be significantly different between these groups ($F=142.87$, $P<0.001$). Ferritin increased in the F (335.30±44.10 μg/l) and F+OVX (324.80±38.60 μg/l) groups compared with the Con (39.40±3.81 μg/l) and OVX (41.38±5.56 μg/l) groups ($P<0.001$, $P<0.001$) (Fig. 1D).

To evaluate the effects of E_2 and FAC on bone metabolism, micro-CT analyses of trabecular and cortical bone were performed. As expected, the excess iron in the F+OVX group (absence of estrogen) markedly reduced both trabecular and cortical bone compared with the OVX group, whereas the Con and F groups (presence of estrogen) showed no significant difference in these parameters except Tb.Sp (Table 2). No significant differences were observed for the Tb.N, SMI, and cortical indexes. These data indicated that estrogen played a key role in suppressing iron-induced bone loss. Three-dimensional reconstruction images are shown in Fig. 2A.

Oxidative stress was evaluated by measuring the levels of MDA and SOD, two commonly used indicators of ROS levels. We compared MDA and SOD in ovariectomized and sham-operated mice that had been administered FAC and normal saline. Differences were significant (MDA: $F=19.62$, $P<0.001$; SOD: $F=22.73$, $P<0.001$). FAC was shown to promote the generation of ROS in ovariectomized mice (MDA: 8.46±1.91 versus 16.14±2.42 nM, $P=0.004$; SOD: 4.43±0.81 versus 1.80±0.67 U/m, $P<0.001$, OVX versus F+OVX), whereas the presence of estrogen suppressed oxidative stress (MDA: 6.22±1.38 versus 8.14±2.06 nM, $P=0.182$; SOD: 5.83±0.77 versus 4.73±0.93 U/ml, $P=0.081$, Con versus F) (Fig. 2B and C).

To further investigate bone turnover, sera were analyzed using ELISA kits. The levels of two factors involved in bone resorption, TRAP5b and CTX, were significantly different (TRAP5b: $F=140.08$, $P<0.001$; CTX: $F=266.93$, $P<0.001$). We observed higher levels of TRAP5b and CTX in the F+OVX group than in the OVX group (TRAP5b: 60.15±3.49 versus 79.04±6.47 U/l, $P<0.001$; CTX: 9624±1140 versus 14506±915 pmol/l, $P<0.001$,OVX versus F+OVX). However, the presence of estrogen abrogated this effect. In accordance with the results of the micro-CT analysis, no significant differences were observed between the Con and F groups (TRAP5b: 23.27±5.66 versus 29.51±5.65 U/l, $P=0.085$; CTX: 2588±662 versus 3633±

http://joe.endocrinology-journals.org
DOI: 10.1530/JOE-14-0657

Published by Bioscientifica Ltd.

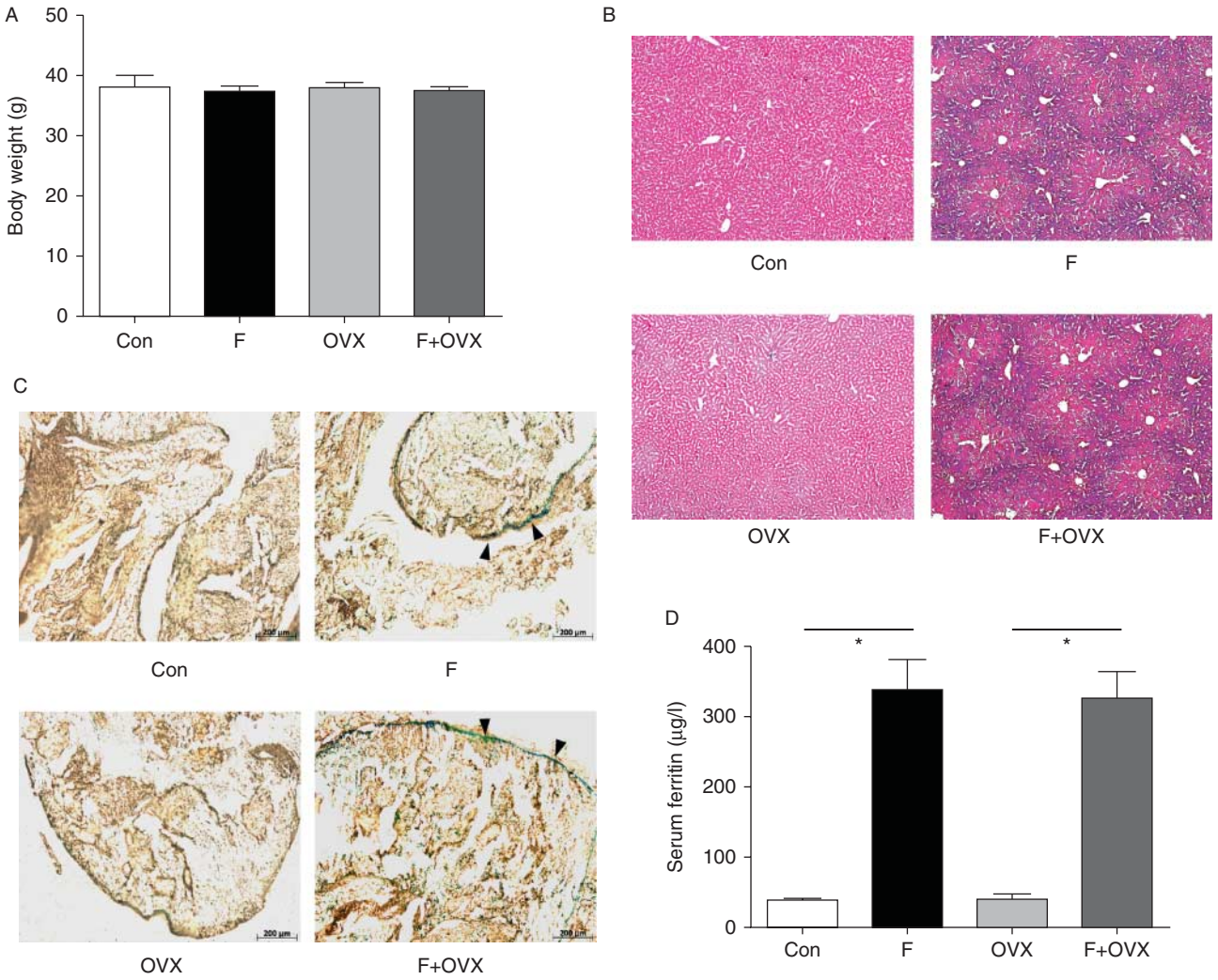

Figure 1
Body weight and iron accumulation in our *in vivo* mouse model. Mice received i.p. injections of normal saline or FAC with or without ovariotomy for 2 months. (A) Body weight was noted to exclude this interference factor. (B) Livers were decalcified and embeded in paraffin and stained with prussian blue. (C) Undecalcified distal femurs were embeded in resin. Iron accumulation level was observed with Prussian blue staining. Iron was deposited in the cortical surface (arrows). (D) The serum ferritin was examined using an ELISA kit. The bar graph represents means±S.D. The asterisks (*) indicate significant differences at $P<0.05$. A full colour version of this figure is available at http://dx.doi.org/10.1530/JOE-14-0657.

449 pmol/l, $P=0.065$, Con versus F) (Fig. 2D and E). We also assessed ALP and osteocalcin levels in each group (ALP: $F=30.69$, $P<0.001$; osteocalcin: $F=69.93$, $P<0.001$). Iron reduced ALP and osteocalcin in both ovariectomized (ALP: 17.57±2.09 versus 11.65±2.02 U/100 ml, $P<0.001$; osteocalcin: 98.27±7.00 versus 83.06±4.46 ng/ml, $P=0.002$, OVX versus F+OVX) and sham-operated (ALP: 14.15±1.22 versus 8.47±1.30 U/100 ml, $P<0.001$; osteocalcin: 73.33±3.85 versus 57.75±3.95 ng/ml, $P<0.001$, Con versus F) mice, indicating that estrogen improved iron-induced osteopenia during the process of bone resorption, but not during bone formation (Fig. 2F and G).

Iron-induced defects in bone formation were not attenuated by estrogen

We investigated activation of varieties of deionized-water-treated and FAC-treated OBs in the presence of E_2 or vehicle. ALP staining and ALP activity assays indicated that ALP activity was significantly different ($F=23.63$, $P<0.001$) and the exposure of FAC-treated OBs to vehicle affected ALP activity (1.34±0.08 versus 0.49±0.17 U/gprot, deionized water-treated versus FAC-treated, $P=0.015$), as had been reported previously (Yamasaki & Hagiwara 2009). To validate our *in vivo* findings, we added FAC to the culture

Table 2 Micro-CT analysis of mice trabecular and cortical bone ($n=6$)[a]

Indexes	Con	F	OVX	F+OVX	*F*	*P*
Trabecular bone						
BMD (mg/mm^3)	0.19±0.06	0.19±0.03	0.11±0.01	0.09±0.06[b]	8.10	0.001
BV/TV (%)	20.37±2.62	17.51±3.37	10.60±1.61	7.07±0.30[b]	43.03	<0.001
Tb.Th (μm)	95.94±6.00	95.98±3.24	89.40±0.49	80.46±4.72[b]	18.73	<0.001
Tb.Sp (μm)	284.60±9.74	337.56±22.95[c]	503.38±62.81	657.59±24.74[b]	132.7	<0.001
Tb.Pf (1/mm)	6.81±0.83	7.38±1.08	13.32±0.91	17.46±0.49[b]	212.2	<0.001
Tb.N (1/mm)	2.131±0.522	1.926±1.080	1.110±0.220	0.879±0.014	5.88	0.005
SMI	1.840±0.239	1.947±0.107	2.296±0.083	2.396±0.008	22.83	<0.001
Cortical bone						
Volume (mm^3)	1.135±0.018	1.167±0.166	1.177±0.034	1.210±0.064	0.69	0.568
Surface (mm^2)	12.102±0.002	12.143±0.753	12.396±0.529	12.601±0.639	1.04	0.396
Thickness (mm)	0.194±0.009	0.209±0.015	0.173±0.006	0.151±0.003[b]	43.64	<0.001

Con, control group; F: mice treated with FAC; OVX: mice treated with ovariotomy; F+OVX: mice treated with FAC and ovariotomy; BMD, bone mineral density; BV/TV, bone volume/total volume; Tb.Th, trabecular thickness; Tb.Sp, trabecular separation; Tb.Pf, trabecular bone pattern factor; Tb.N, trabecular number; SMI, structure model index.
[a]FAC markedly reduced trabecular bone mass and significantly affected other related parameters on the basis of ovariotomy. While the indices of mice without ovariotomy were rarely affected by iron.
[b]Significant difference with OVX group ($P<0.05$).
[c]Significant difference with Con group ($P<0.05$).

medium containing E_2. In comparison with the cells treated with E_2 alone, the cells co-incubated in FAC and E_2 had lower ALP activity (1.49±0.20 versus 0.76±0.20 U/gprot, E_2-treated versus FAC&E_2-treated, $P=0.021$) (Fig. 3A and B). Alizarin red staining provided us with a result that FAC inhibited OBs mineralization ability with or without estrogen. (Fig. 3C)

Quantitative RT-PCR analysis of *RUNX2*, *SP7*, and *BGLAP* mRNA levels confirmed the ALP analysis results, demonstrating that iron-induced changes in mRNA levels were not attenuated by E_2 (*RUNX2*: $F=9.21$, $P=0.029$, *SP7*: $F=15.56$, $P=0.011$; *BGLAP*: $F=7.20$, $P=0.043$). FAC decreased *RUNX2*, *SP7*, and *BGLAP* expression, and the fold-decreases of these mRNAs, 0.24-, 0.69- and 0.72-fold

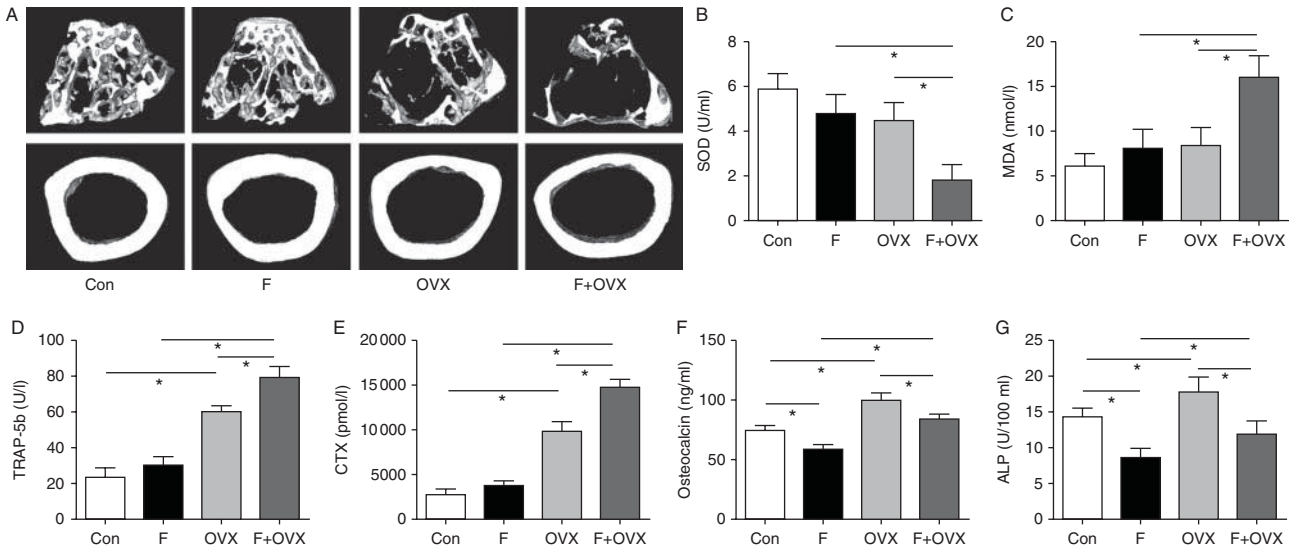

Figure 2
Micro-CT three-dimensional reconstruction images and evaluation of oxidative stress, bone resorption, and bone formation markers *in vivo*. (A) Micro-CT images of mice belonging to the Con, F, OVX, and F+OVX groups. The trabecular bone of the distal femur and cortical bone of the mid-diaphysis femur are shown. (B and C) Levels of the oxidative stress markers superoxide dismutase (SOD) and malondialdehyde (MDA). (D and E) Serum levels of the bone resorption markers tartrate resistant acid phosphatase (Trap5b) and C-terminal telopeptide of type 1 collagen (CTX). (F and G) Serum levels of osteocalcin and alkaline phosphatase (ALP) were evaluated as markers of bone formation. The bar graphs show the means±S.D. The asterisks (*) indicate significant differences at $P<0.05$.

http://joe.endocrinology-journals.org
DOI: 10.1530/JOE-14-0657

Published by Bioscientifica Ltd.

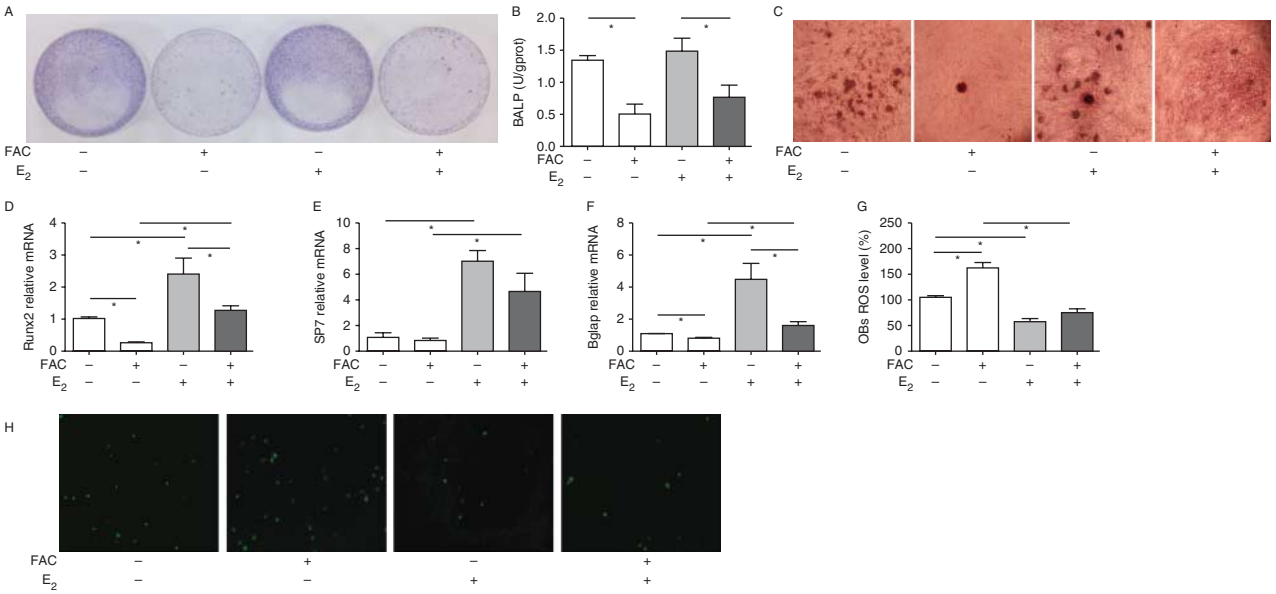

Figure 3

Relative biological function of OBs. (A) ALP staining of osteoblasts (OBs). (B) The level of ALP activity in OBs. ALP activity and protein concentration in supernatants were measured using an ALP activity assay kit. (C) Alizarin red staining of OBs (40× magnification). (D, E and F) Quantitative real-time polymerase chain reaction (RT-PCR) analysis of the expression of bone formation markers including runt related transcription factor 2 (*RUNX2*), transcription factor *SP7*, and bone γ gamma carboxyglutamate acid containing protein (*BGLAP*). (G and H) The effect of FAC on the generation of reactive oxygen species (ROS) in OBs in the presence and absence of estradiol (E_2) (100× magnification). The bar graphs show the means±S.D. *$P<0.05$ indicates a statistically significant difference. A full colour version of this figure is available at http://dx.doi.org/10.1530/JOE-14-0657.

($P=0.036$, 0.481, 0.049 respectively), were significantly different from that of the deionized water control. When E_2 was added to the wells, the FAC-induced fold-changes decreased to 0.52-, 0.66- and 0.35-fold ($P=0.020$, 0.292, 0.050 respectively) (Fig. 3D, E and F). Therefore, our quantitative RT-PCR analysis generated data that were consistent with that from the animal experiments.

Next, we determined the levels of ROS in each group. Because cellular ROS reportedly decreases in response to E_2 and promotes apoptosis of OBs, we investigated whether FAC could influence oxidative stress in the presence and absence of E_2. The cultures were treated and the production rate of ROS was then assessed using the fluorescent probe DCFH-DA. As shown in Fig. 3G and H, the production rate of ROS was significantly different ($F=37.44$, $P<0.001$). ROS increased significantly in response to 10-μM FAC treatment (100.00±10.36 versus 156.30±24.57%, deionized water-treated versus FAC-treated, $P<0.001$), but this effect was attenuated in cells that were pretreated in 10 nM E_2 (54.16±14.90 vs 76.06±19.09%, E_2-treated versus FAC&E_2-treated, $P=0.142$). These data supported the conclusions of the *in vivo* experiments. However, they varied from the results of the quantitative RT-PCR analysis of OBs. Briefly speaking, though E_2 attenuated the iron-induced ROS level, iron-induced reduction in activation of OBs could not be improved by E_2.

Inhibitory effect of estrogen on osteoclast differentiation in the presence of iron

Because the iron-induced defects in bone formation could not be attenuated by estrogen, we next explored the combined actions of estrogen and iron on bone resorption by evaluating the effects of FAC and E_2 on osteoclast activation. Various concentrations of FAC (0, 12, 25, 50, 100, and 200 μM) and E_2 (0, 1, 10, 10^2, 10^3, and 10^4 nM) were applied to RAW264.7 cells in the presence of 100 ng/ml of RANKL. As indicated by the number of Trap-positive MNCs, though higher concentrations of FAC and E_2 inhibited proliferation of the cells (Fig. 4A and B), differentiation of RAW264.7 cells was stimulated with the indicated doses of FAC (50 μM) ($P<0.001$) and inhibited with the indicated doses of E_2 (10 nM) ($P=0.001$) (Fig. 4C and D). These doses were used during the subsequent experiments.

The number of Trap-positive MNCs in cultures treated with both FAC and E_2 was also scored ($F=43.19$, $P<0.001$). Preliminary results indicated that FAC could only promote osteoclast differentiation in the absence of

http://joe.endocrinology-journals.org
DOI: 10.1530/JOE-14-0657

Published by Bioscientifica Ltd.

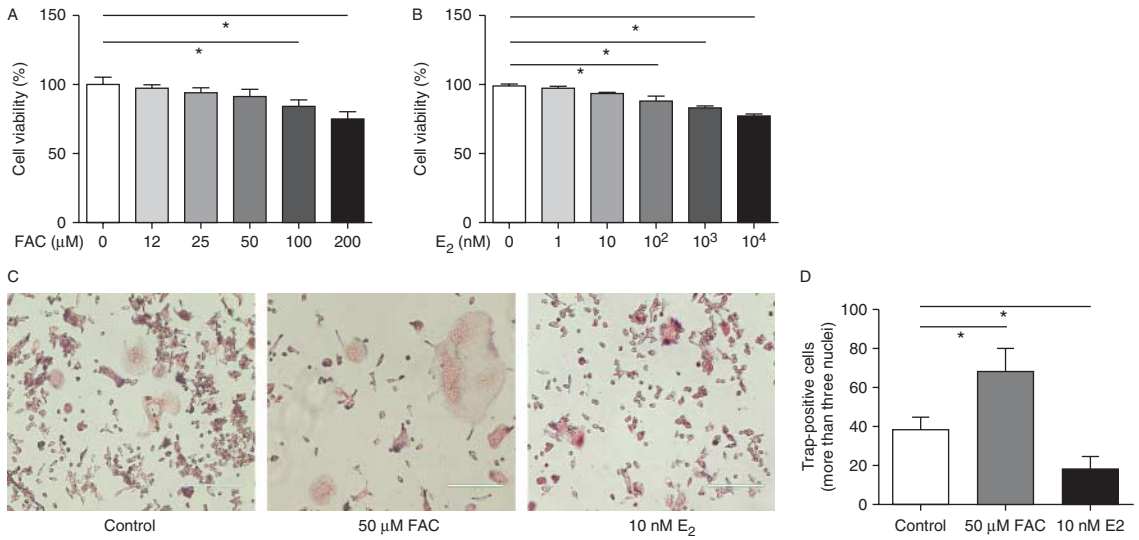

Figure 4

Cell viability and the effects of E_2 and FAC on RAW264.7 cells pretreated with RANKL. (A and B) Cell Counting kit 8 (CCK8) was used to test cell viability. (C and D) Trap staining of RAW264.7 cells in medium containing the indicated concentrations of E_2 and FAC and 100 ng/ml receptor activator of NF-kB ligand (RANKL) (200× magnification). Wine red cells (Trap-positive cells) containing three or more nuclei were considered to be osteoclasts. The numbers of wine red cells were quantified. The bar graph shows the means±s.d. *$P<0.05$ indicates a statistically significant difference. A full colour version of this figure is available at http://dx.doi.org/10.1530/JOE-14-0657.

E_2 (37.80±7.22 versus 67.33±12.40, deionized water-treated versus FAC-treated, $P<0.001$; 17.33±6.71 versus 22.50±5.09, E_2-treated versus FAC&E_2-treated, $P=0.299$) (Fig. 5A and B), a finding consistent with the results of our resorption pit assay, including number of pits ($F=316.50$, $P<0.001$) and area ratio ($F=61.13$, $P<0.001$) (Fig. 5C, D and E). BMMs isolated from femurs were cultured and then Trap stained. The number of Trap-positive MNCs was significantly different between the four groups ($F=92.24$, $P<0.001$). The number for the F+OVX group was significantly greater than that for the OVX group (12.67±1.75 versus 19.67±3.08, OVX versus F+OVX, $P<0.001$). However, the presence of estrogen partly abrogated iron-induced osteoclast differentiation (2.33±1.75 versus 3.17±1.47, Con versus F, $P=0.501$) (Fig. 5F and G). This result supports our hypothesis that estrogen ameliorates iron-induced bone loss during the process of bone resorption, but not bone formation.

We used the fluorescent probe DCFH-DA to determine whether iron or estrogen changed intracellular ROS levels. As expected, the results of this experiment were consistent with the results for detection of ROS in OBs, as shown in Fig. 6A and B ($F=55.66$, $P<0.001$). We examined whether iron and estrogen affected osteoclast differentiation by measuring *TRAP*, *CTSK*, *MMP9*, and *CALCR* expression. As shown in Fig. 6C, D, E and F (*TRAP*: $F=7.12$, $P=0.044$, *CTSK*: $F=9.92$, $P=0.025$; *MMP9*: $F=16.00$, $P=0.011$, *CALCR*: $F=13.50$, $P=0.015$), the expression levels in iron-treated cells were significantly higher than in cells treated with deionized water, increasing by 2.49-, 4.82-, 3.31-, and 9.19-fold, respectively ($P=0.047$, 0.036, 0.046, <0.001 respectively). Unexpectedly, compared with cells treated with estrogen alone, the expression of *TRAP*, *CTSK*, *MMP9*, and *CALCR* displayed no obvious differences in the cells treated with estrogen and iron (1.27-, 2.06-, 2.24-, and 3.68-fold respectively) ($P=0.741$, 0.274, 0.386, 0.201 respectively). To further elucidate this mechanism, we extracted nuclear and cytoplasmic proteins and performed a western blot analysis. Nuclear proteins P65 and P50 and cytoplasmic proteins IkBα and phosphorylated IkBα were examined ($F=59.52$, 41.81, 38.92, 78.21, respectively; $P<0.001$, <0.001, <0.001, <0.001 respectively). No significant change of P65, P50, IkBα and PIkBα activation was observed if cells were treated with E_2 ($P=0.091$, 0.109, 0.258, 0.149 respectively). Whereas IkBα, phosphorylated IkBα, P65, and P50 were obviously affected by iron in the absence of E_2 ($P=0.001$, <0.001, <0.001, 0.007 respectively) (Fig. 6G and H).

Discussion

Postmenopausal osteoporosis, which is characterized by decreased bone mass and microarchitectural deterioration of bone tissue, represents an increasing medical and socioeconomic threat in the aged population worldwide.

http://joe.endocrinology-journals.org
DOI: 10.1530/JOE-14-0657

Published by Bioscientifica Ltd.

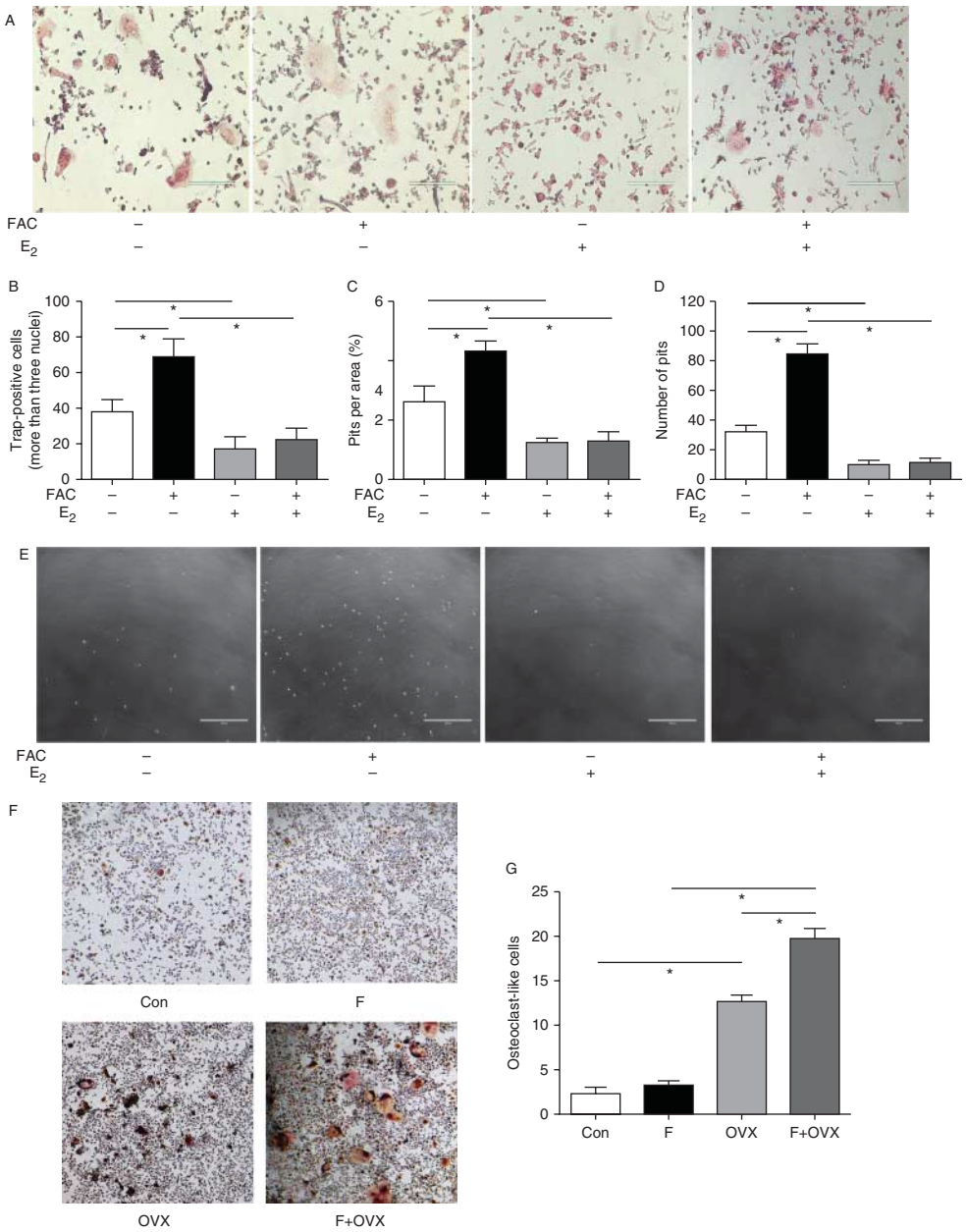

Figure 5

E_2 abrogated the stimulatory effect of FAC on osteoclast differentiation. (A and B) RAW264.7 cells were treated with FAC and E_2 as indicated and Trap stained (200× magnification). Wine red Trap-positive cells were scored. (C, D and E) The effect of FAC and E_2 on bone resorption. The eroded area and the number of pits were shown. (F and G) Bone-marrow-derived macrophages (BMMs) were cultured in the presence of 50 ng/ml RANKL and 30 ng/ml macrophage colony-stimulating factor (M-CSF) for 5 days and subjected to Trap staining to observe osteoclast formation (100× magnification). Wine red cells were considered to be mononucleated cells (MNCs). The bar graph shows the means±S.D. *$P<0.05$ indicates a statistically significant difference. A full colour version of this figure is available at http://dx.doi.org/10.1530/JOE-14-0657.

In addition to estrogen deficiency, iron accumulation has recently been reported to be a secondary causative factor involved in PMO (Jia *et al.* 2012, Li *et al.* 2012, He *et al.* 2013, Kim *et al.* 2013). Postmenopausal women with abnormally high iron are reportedly more susceptible to osteoporosis (Kim *et al.* 2012, 2013). However, whether iron accumulation affects bone metabolism in premenopausal women has not, to our knowledge, been examined. This prompted us to ask whether an excess of iron leads to bone loss in the presence of estrogen.

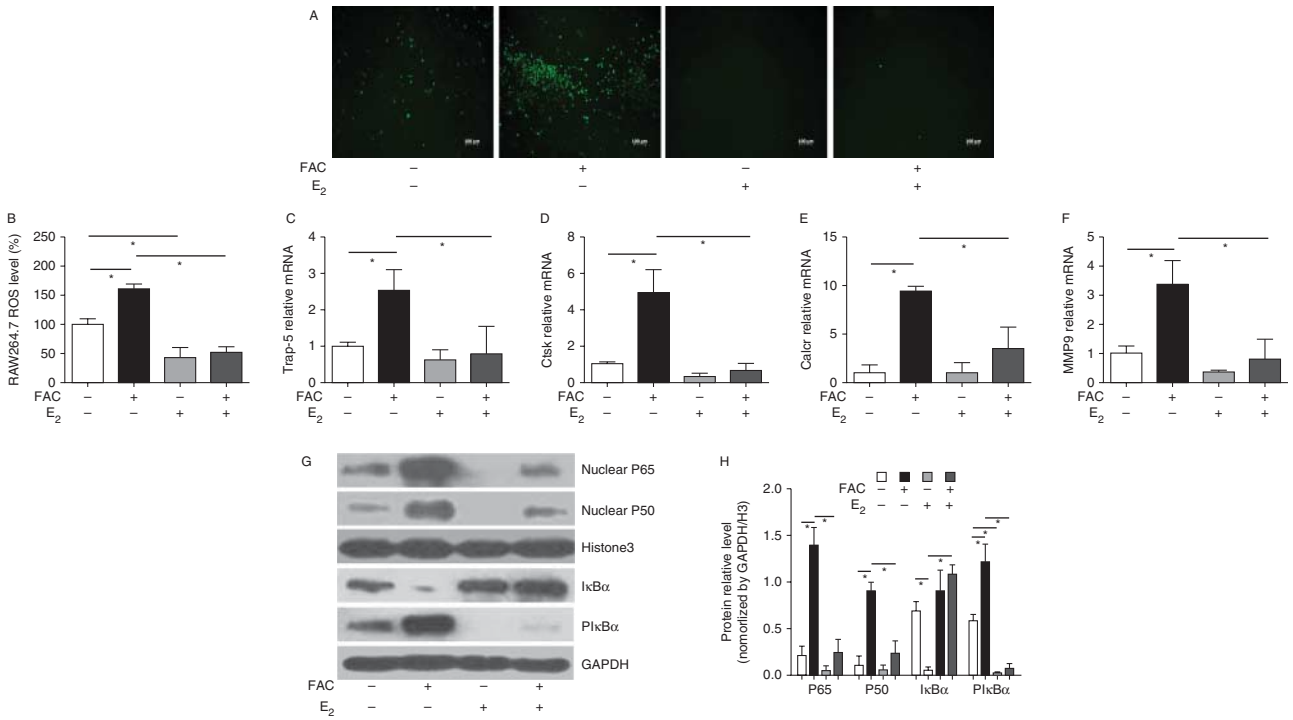

Figure 6

FAC increased and E_2 decreased RANKL-induced gene expression, ROS levels, and NF-κB activation. (A and B) FAC enhanced the production of ROS in RAW264.7 cells only in the absence of E_2 (100× magnification). (C, D, E and F) Quantitative RT-PCR measuring the expression levels of bone formation markers including *TRAP5*, cathepsin K (*CTSK*), calcitonin receptor (*CALCR*), and matrix metallopeptidase 9 (*MMP9*). (G and H) Nuclear and cytoplasmic protein levels were analyzed by western blot. The bar graph shows the means±s.d. $*P<0.05$ indicates a statistically significant difference. A full colour version of this figure is available at http://dx.doi.org/10.1530/JOE-14-0657.

In this study, we generated an OVX mouse model with elevated iron to replicate the characteristic of postmenopausal females. Body weight had an influence on bone mass. The ratio of weight gain in OVX mice was slowed down with a control diet. Our mouse model had a pronounced bone phenotype, with defects similar to the OVX mouse model with normal levels of iron. Defects included trabecular and cortical thinning and alterations in the material properties of the bones. Considering the individual differences between mice and the tiny amounts of samples, levels of Tb.Sp in F group were increased and no significant difference was observed in Tb.N, SMI, cortical volume, surface, or thickness. In spite of these results, changes of other parameters were in accordance with theoretical analysis. In addition, a significant decrease in bone formation and resorption activities were observed in our model, recapitulating iron-induced osteopenia in ovariectomized mice. Similar results have been reported by Jia *et al.* (2012) and Tsay *et al.* (2010).

We also established an iron-accumulation mouse model that was not ovariectomized. In contrast to our OVX model, these mice experienced minimal bone loss, indicating a central role for the bioavailability of estrogen in attenuating iron-induced bone turnover. Interestingly, serum levels of bone formation markers were not consistent with the results of the micro-CT analysis, while those of bone resorption markers were consistent. Based on these findings, we investigated whether estrogen played a key role in protecting OB activity or affecting osteoclast differentiation *in vitro*. Expression of *RUNX2* and SP7 decreased in iron-treated OBs in both the presence and absence of estrogen. In order to determine the dose of FAC and E_2, we generated dose-response curves before performing experiments on osteoclasts. We found that FAC affected differentiation of osteoclasts at a concentration of 50 μM. The concentration for E_2 was 10 nM. We also found that the differentiation of BMMs and RAW264.7 cells could not be stimulated using FAC when estrogen was present. Therefore, we proposed the hypothesis that estrogen protected mice from iron-induced osteopenia by influencing osteoclast differentiation, but not OB activity.

Estrogen is the predominant female steroid hormone and a pivotal regulator in bone formation and bone resorption processes (Chokalingam *et al.* 2012).

http://joe.endocrinology-journals.org
DOI: 10.1530/JOE-14-0657

Published by Bioscientifica Ltd.

Menopausal women have been found to have increased ferritin levels, revealing a possible relationship between estrogen and iron (Jian *et al*. 2009, Ikeda *et al*. 2012, Yang *et al*. 2012). However, our results indicated that serum ferritin levels in the Con and OVX groups did not differ significantly. Thus, estrogen might not act directly on iron metabolism. As previously reported, ROS might be involved in the process of osteopenia induced by iron accumulation (Tsay *et al*. 2010). The mechanisms responsible, such as ROS regulation, should be further investigated. Though E_2 eliminated iron-induced free radicals in OBs, FAC suppressed the activity of OBs in the presence of estrogen. This might indicate that iron-induced ROS are not a major factor mediating the inhibition of the activity of OBs.

Oxidative stress occurs in a cellular system when the production of free radical moieties exceeds the antioxidant capacity of that system. An increase in ROS levels may constitute a stress signal that stimulates specific redox-sensitive signaling pathways (Baek *et al*. 2010). As previously reported, the IκB/p-Tyr, Ras/mitogen-activated protein kinases/NF-κB or protein tyrosine kinase/phospholipase C/NF-κB pathways might be involved in ROS-induced NF-κB regulation (Trushin *et al*. 1999, Ye *et al*. 2000, Siomek 2012). Importantly, NF-κB controls the differentiation or activity of the major skeletal cell types, including osteoclasts, OBs, osteocytes, and chondrocytes (Alles *et al*. 2010, Novack 2011). NF-κB is a transcription factor that forms either homo- or heterodimers with various members of the Rel family, such as P50, P52, P65, cRel, and RelB. Together, they regulate the expression of numerous genes that are critical for the regulation of apoptosis, inflammation, viral replication, and various autoimmune diseases (Mankan *et al*. 2009, Hua *et al*. 2012). NF-κB, inhibited by its interaction with IκBa, IκBβ, IκBγ, and IκBε, is sequestered in the cytoplasm (Dyson & Komives 2012). Based on the results of this study, we speculate that iron-induced production of ROS leads to the phosphorylation of IκB and activates NF-κB (P50-P65 heterodimer), exposing a subunit of NF-κB (P50) and inducing nuclear translocation (Pereira & Oakley 2008). Nuclear P65, another subunit of NF-κB, binds to the consensus sequence of various genes, thus activating their transcription (Vermeulen *et al*. 2002). Therefore, the NF-κB pathway plays a fundamental role in the process of osteoclast differentiation (Soysa & Alles 2009, Novack 2011).

In summary, our data provided evidence supporting the conclusion that ROS, generated by iron, stimulated differentiation of osteoclasts, while estrogen inhibited iron-induced osteopenia by eliminating ROS in osteoclasts. Our results provided evidence indicative of a unique role of iron in pre- or post-menopausal osteoporosis. Drugs such as an iron chelator might be a potential treatment for PMO in the future. A weakness might be the size of the FAC dose, which induced a six- to sevenfold higher peak in iron levels than that of non-iron-treated mice. While in humans, the ratio is only two- to threefold (Huang *et al*. 2013). Species differences must be taken into account when considering the relationship between severity of iron excess and development of osteopenia. Non-canonical NF-κB signaling has not been considered. It will be examined in our follow-up experiment. A major strength of this study was that our mouse model reasonably recapitulated many features of postmenopausal women who have elevated iron levels. Furthermore, we used combined treatment with estrogen and iron to elucidate the effects of iron on bone metabolism.

Declaration of interest

The authors declare that there is no conflict of interest that could be perceived as prejudicing the impartiality of the research reported.

Funding

This study was supported by The National Natural Science Foundation of China (no. 81273090 and no. 81302438), Jiangsu Provincial Grant (no. BL2014044), Study on the Project Application of Suzhou (LCZX210305), and Science and Technology Projects of Suzhou (SS201327).

Author contribution statement

Operation of experiments: W Xiao and F Beibei. Drafting the paper: S Guangsi. Data statistics: J Yu. Provision of instruments: Z Wen. Design of this research: H Xi and X Youjia. All authors have read and approved the final submitted manuscript.

Acknowledgements

We are grateful to the animal care committee of Soochow University for logistical support and to the Commission for Science and Technology. Sincere thanks to Sun Jingyue and Wang Sheng for their help with laboratory work. Yu Chen provided important assistance with the figures. Zhang Peng and Li Guangfei offered valuable editorial advice.

References

Alles N, Soysa NS, Hayashi J, Khan M, Shimoda A, Shimokawa H, Ritzeler O, Akiyoshi K, Aoki K & Ohya K 2010 Suppression of NF-κB increases bone formation and ameliorates osteopenia in ovariectomized mice. *Endocrinology* **151** 4626–4634. (doi:10.1210/en.2010-0399)

Baek KH, Oh KW, Lee WY, Lee SS, Kim MK, Kwon HS, Rhee EJ, Han JH, Song KH, Cha BY *et al*. 2010 Association of oxidative stress with postmenopausal osteoporosis and the effects of hydrogen peroxide on osteoclast formation in human bone marrow cell cultures. *Calcified Tissue International* **87** 226–235. (doi:10.1007/s00223-010-9393-9)

http://joe.endocrinology-journals.org
DOI: 10.1530/JOE-14-0657

Published by Bioscientifica Ltd.

Chinese Orthopaedic Association 2009 Diagnosis and treatment of osteoporotic fractures. *Orthopaedic Surgery* **1** 251–257. (doi:10.1111/j.1757-7861.2009.00047.x)

Chokalingam K, Roforth MM, Nicks KM, McGregor U, Fraser D, Khosla S & Monroe DG 2012 Examination of ERα signaling pathways in bone of mutant mouse models reveals the importance of ERE-dependent signaling. *Endocrinology* **153** 5325–5333. (doi:10.1210/en.2012-1721)

Dyson HJ & Komives EA 2012 Role of disorder in IκB-NFκB interaction. *IUBMB Life* **64** 499–505. (doi:10.1002/iub.1044)

Guggenbuhl P, Deugnier Y, Boisdet JF, Rolland Y, Perdriger A, Pawlotsky Y & Chales G 2005 Bone mineral density in men with genetic hemochromatosis and HFE gene mutation. *Osteoporosis International* **16** 1809–1814. (doi:10.1007/s00198-005-1934-0)

Ha H, Kwak HB, Lee SW, Jin HM, Kim HM, Kim HH & Lee ZH 2004 Reactive oxygen species mediate RANK signaling in osteoclasts. *Experimental Cell Research* **301** 119–127. (doi:10.1016/j.yexcr.2004.07.035)

He YF, Ma Y, Gao C, Zhao GY, Zhang LL, Li GF, Pan YZ, Li K & Xu YJ 2013 Iron overload inhibits osteoblast biological activity through oxidative stress. *Biological Trace Element Research* **152** 292–296. (doi:10.1007/s12011-013-9605-z)

Hohn A, Konig J & Grune T 2013 Protein oxidation in aging and the removal of oxidized proteins. *Journal of Proteomics* **92** 132–159. (doi:10.1016/j.jprot.2013.01.004)

Hua R, Pease JE, Sooranna SR, Viney JM, Nelson SM, Myatt L, Bennett PR & Johnson MR 2012 Stretch and inflammatory cytokines drive myometrial chemokine expression via NF-κB activation. *Endocrinology* **153** 481–491. (doi:10.1210/en.2011-1506)

Huang X, Xu Y & Partridge NC 2013 Dancing with sex hormones, could iron contribute to the gender difference in osteoporosis? *Bone* **55** 458–460. (doi:10.1016/j.bone.2013.03.008)

Ikeda Y, Tajima S, Izawa-Ishizawa Y, Kihira Y, Ishizawa K, Tomita S, Tsuchiya K & Tamaki T 2012 Estrogen regulates hepcidin expression via GPR30-BMP6-dependent signaling in hepatocytes. *PLoS ONE* **7** e40465. (doi:10.1371/journal.pone.0040465)

Jia P, Xu YJ, Zhang ZL, Li K, Li B, Zhang W & Yang H 2012 Ferric ion could facilitate osteoclast differentiation and bone resorption through the production of reactive oxygen species. *Journal of Orthopaedic Research* **30** 1843–1852. (doi:10.1002/jor.22133)

Jian J, Pelle E & Huang X 2009 Iron and menopause: does increased iron affect the health of postmenopausal women? *Antioxidants & Redox Signaling* **11** 2939–2943. (doi:10.1089/ars.2009.2576)

Khosla S, Oursler MJ & Monroe DG 2012 Estrogen and the skeleton. *Trends in Endocrinology and Metabolism* **23** 576–581. (doi:10.1016/j.tem.2012.03.008)

Kim JK, Pedram A, Razandi M & Levin ER 2006 Estrogen prevents cardiomyocyte apoptosis through inhibition of reactive oxygen species and differential regulation of p38 kinase isoforms. *Journal of Biological Chemistry* **281** 6760–6767. (doi:10.1074/jbc.M511024200)

Kim BJ, Ahn SH, Bae SJ, Kim EH, Lee SH, Kim HK, Choe JW, Koh JM & Kim GS 2012 Iron overload accelerates bone loss in healthy postmenopausal women and middle-aged men: a 3-year retrospective longitudinal study. *Journal of Bone and Mineral Research* **27** 2279–2290. (doi:10.1002/jbmr.1692)

Kim BJ, Lee SH, Koh JM & Kim GS 2013 The association between higher serum ferritin level and lower bone mineral density is prominent in women ≧45 years of age (KNHANES 2008–2010). *Osteoporosis International* **24** 2627–2637. (doi:10.1007/s00198-013-2363-0)

Krum SA, Miranda-Carboni GA, Hauschka PV, Carroll JS, Lane TF, Freedman LP & Brown M 2008 Estrogen protects bone by inducing Fas ligand in osteoblasts to regulate osteoclast survival. *Embo Journal* **27** 535–545. (doi:10.1038/sj.emboj.7601984)

Lee NK, Choi YG, Baik JY, Han SY, Jeong DW, Bae YS, Kim N & Lee SY 2005 A crucial role for reactive oxygen species in RANKL-induced osteoclast differentiation. *Blood* **106** 852–859. (doi:10.1182/blood-2004-09-3662)

Li GF, Pan YZ, Sirois P, Li K & Xu YJ 2012 Iron homeostasis in osteoporosis and its clinical implications. *Osteoporosis International* **23** 2403–2408. (doi:10.1007/s00198-012-1982-1)

Mahachoklertwattana P, Sirikulchayanonta V, Chuansumrit A, Karnsombat P, Choubtum L, Sriphrapradang A, Domrongkitchaiporn S, Sirisriro R & Rajatanavin R 2003 Bone histomorphometry in children and adolescents with β-thalassemia disease: iron-associated focal osteomalacia. *Journal of Clinical Endocrinology and Metabolism* **88** 3966–3972. (doi:10.1210/jc.2002-021548)

Mankan AK, Lawless MW, Gray SG, Kelleher D & McManus R 2009 NF-κB regulation: the nuclear response. *Journal of Cellular and Molecular Medicine* **13** 631–643. (doi:10.1111/j.1582-4934.2009.00632.x)

Matsushima S, Hoshimoto M, Torii M, Ozaki K & Narama I 2001 Iron lactate-induced osteopenia in male Sprague–Dawley rats. *Toxicologic Pathology* **29** 623–629. (doi:10.1080/019262301753385951)

Messer JG, Kilbarger AK, Erikson KM & Kipp DE 2009 Iron overload alters iron-regulatory genes and proteins, down-regulates osteoblastic phenotype, and is associated with apoptosis in fetal rat calvaria cultures. *Bone* **45** 972–979. (doi:10.1016/j.bone.2009.07.073)

Milman N & Kirchhoff M 1992 Iron stores in 1359, 30- to 60-year-old Danish women: evaluation by serum ferritin and hemoglobin. *Annals of Hematology* **64** 22–27. (doi:10.1007/BF01811467)

Nakrst J, Bistan M, Tisler T, Zagorc-Koncan J, Derco J & Gotvajn AZ 2011 Comparison of Fenton's oxidation and ozonation for removal of estrogens. *Water Science and Technology* **63** 2131–2137. (doi:10.2166/wst.2011.339)

Novack DV 2011 Role of NF-κB in the skeleton. *Cell Research* **21** 169–182. (doi:10.1038/cr.2010.159)

Pereira SG & Oakley F 2008 Nuclear factor-κB1: regulation and function. *International Journal of Biochemistry & Cell Biology* **40** 1425–1430. (doi:10.1016/j.biocel.2007.05.004)

Ray NF, Chan JK, Thamer M & Melton LJ III 1997 Medical expenditures for the treatment of osteoporotic fractures in the United States in 1995: report from the National Osteoporosis Foundation. *Journal of Bone and Mineral Research* **12** 24–35. (doi:10.1359/jbmr.1997.12.1.24)

Riggs BL, Khosla S & Melton LJ III 2002 Sex steroids and the construction and conservation of the adult skeleton. *Endocrine Reviews* **23** 279–302. (doi:10.1210/edrv.23.3.0465)

Ross PD 1996 Osteoporosis, frequency, consequences and risk factors. *Archives of Internal Medicine* **156** 1399–1411. (doi:10.1001/archinte.1996.00440120051005)

Siomek A 2012 NF-κB signaling pathway and free radical impact. *Acta Biochimica Polonica* **59** 323–331.

Soysa NS & Alles N 2009 NF-κB functions in osteoclasts. *Biochemical and Biophysical Research Communications* **378** 1–5. (doi:10.1016/j.bbrc.2008.10.146)

Suda T, Jimi E, Nakamura I & Takahashi N 1997 Role of 1 α,25-dihydroxy-vitamin D_3 in osteoclast differentiation and function. *Methods in Enzymology* **282** 223–235. (doi:10.1016/S0076-6879(97)82110-6)

Trushin SA, Pennington KN, Algeciras-Schimnich A & Paya CV 1999 Protein kinase C and calcineurin synergize to activate IκB kinase and NF-κB in T lymphocytes. *Journal of Biological Chemistry* **274** 22923–22931. (doi:10.1074/jbc.274.33.22923)

Tsay J, Yang Z, Ross FP, Cunningham-Rundles S, Lin H, Coleman R, Mayer-Kuckuk P, Doty SB, Grady RW, Giardina PJ *et al.* 2010 Bone loss caused by iron overload in a murine model: importance of oxidative stress. *Blood* **116** 2582–2589. (doi:10.1182/blood-2009-12-260083)

Van den Bergh JP, van Geel TA & Geusens PP 2012 Osteoporosis, frailty and fracture: implications for case finding and therapy. *Nature Reviews. Rheumatology* **8** 163–172. (doi:10.1038/nrrheum.2011.217)

Vermeulen L, De Wilde G, Notebaert S, Vanden Berghe W & Haegeman G 2002 Regulation of the transcriptional activity of the nuclear factor-κB p65 subunit. *Biochemical Pharmacology* **64** 963–970. (doi:10.1016/S0006-2952(02)01161-9)

Vogiatzi MG, Macklin EA, Fung EB, Vichinsky E, Olivieri N, Kwiatkowski J, Cohen A, Neufeld E & Giardina PJ 2006 Prevalence of fractures among

http://joe.endocrinology-journals.org
DOI: 10.1530/JOE-14-0657

Published by Bioscientifica Ltd.

the Thalassemia syndromes in North America. *Bone* **38** 571–575. (doi:10.1016/j.bone.2005.10.001)

Yamasaki K & Hagiwara H 2009 Excess iron inhibits osteoblast metabolism. *Toxicology Letters* **191** 211–215. (doi:10.1016/j.toxlet.2009.08.023)

Yang Q, Jian J, Abramson SB & Huang X 2011 Inhibitory effects of iron on bone morphogenetic protein 2-induced osteoblastogenesis. *Journal of Bone and Mineral Research* **26** 1188–1196. (doi:10.1002/jbmr.337)

Yang Q, Jian J, Katz S, Abramson SB & Huang X 2012 17β-Estradiol inhibits iron hormone hepcidin through an estrogen responsive element half-site. *Endocrinology* **153** 3170–3178. (doi:10.1210/en.2011-2045)

Ye J, Ding M, Zhang X, Rojanasakul Y & Shi X 2000 On the role of hydroxyl radical and the effect of tetrandrine on nuclear factor–κB activation by phorbol 12-myristate 13-acetate. *Annals of Clinical Laboratory Science* **30** 65–71.

Received in final form 13 June 2015
Accepted 22 June 2015
Accepted Preprint published online 26 June 2015

http://joe.endocrinology-journals.org
DOI: 10.1530/JOE-14-0657

Published by Bioscientifica Ltd.